| | |
|---|---|
| Title | Preparation of peptide- and protein-based molecular assemblies and their utilizations as nanocarriers for tumor imaging |
| Author(s) | Makino, Akira; Kimura, Shunsaku |
| Citation | Reactive and Functional Polymers (2011), 71(3): 272-279 |
| Issue Date | 2011-03 |
| URL | http://hdl.handle.net/2433/138087 |
| Right | © 2010 Elsevier Ltd |
| Type | Journal Article |
| Textversion | author |

**Preparation of Peptide- and Protein-based Molecular Assemblies and Their Utilizations as Nanocarriers for Tumor Imaging**

Akira Makino and Shunsaku Kimura

Department of Material Chemistry, Graduate School of Engineering, Kyoto University, Kyoto 615-8510, Japan

Corresponding should be addressed to Shunsaku Kimura

Kyoto-Daigaku-Katsura, Nishikyo-ku, Kyoto 615-8510, Japan

Tel: +81-75-383-2400, Fax: +81-75-383-2401, e-mail: shun@scl.kyoto-u.ac.jp

**Abstract**

Three types of nanocarriers from our group for imaging probes are reviewed here. Novel nanocarrierirs of “peptosome” and “lactosome” were prepared from amphiphilic polymers uniquely having a helical segment as a hydrophobic block. Apoferritin was chemically modified on the surface, and used for nanocontainer of a novel Gd-chelator. Lactosome was intensively studied and labeled with indocyanine, $^{18}$F, and $^{131}$I for tumor imaging by NIRF, PET, and SPECT, respectively. Those labeled lactosomes are shown to be effective for tumor imaging on the basis of the EPR effect and the stealth property *in vivo*. The superiority of lactosome over other commercially available imaging agents is experimentally confirmed, which is explained by the dense and thick hydrophilic polymer brush formed on the surface and the helix bundles at the hydrophobic core. Our final goal is to develop the next-generation lactosome, which is the nanocarrier which is usable for a diagnostic agent and a therapeutic agent showing the same *in vivo* disposition even upon frequent administration.

**Keywords**

Molecular assembly, Nanocarriers, Molecular imaging, EPR effect, Cancer diagnosis

## 1. Introduction

Cancer is one of the most common causes of death and 7.9 million of people died of cancer (around 13% of all deaths) in 2007.[1] In order to improve the likelihood of cure and survival rate from cancer, cancer diagnosis at an early stage is essential. Recently, “molecular imaging”, which is an *in vivo* non-invasive visualization technique, is focused on. This technique detects biological phenomena specific to cancers by monitoring the behavior of probes in the living organisms. The technique is therefore spreading widely not only in the fundamental research areas for the elucidations of living system mechanisms, but also in applicative areas such as medicine and pharmaceutics. Various kinds of imaging modalities including computed tomography (CT), magnetic resonance (MR), positron emission tomography (PET), single photon emission computed tomography (SPECT), near-infrared optical imaging (NIRF) and so on, have been developed and utilized on medical purposes. Developments both of new highly sensitive imaging machines and probes including effective contrast agents are necessary for the early detection of cancer by molecular imaging techniques.

To improve the sensitivity for the tumor detection, several strategies have been examined for molecular probes to target actively to tumor regions by using antibody[2] and receptor-oriented ligands.[3,4] On the other hand, the enhanced permeability and retention (EPR) effect, which is one of the well-known techniques, is also widely used for tumor targeting, even though the EPR effect is based on the passive targetting.[5-7] In tumor tissues, submicron-sized defects exist on the vascular wall because of the rapid angiogenesis, enabling permeation of macromolecules through the wall. Further, the lymph system cannot overtake the rapid growth of the tumor, resulted in an inadequate ability to exclude foreign compounds from the tumor region. Accordingly, macromolecules and leukocytes, whose sizes are in the range of ca. 10–100 nm, are considered to be passively accumulated in the tumor region. [5-7]

On the basis of the concept of the EPR effect, various nanocarriers including polymeric micelles and vesicles, protein capsules, carbon nanotubes, dendrimers, quntum dots, and inorganic

nanoparticles have been applied for development of efficient tumor imaging probes.[8-12] We have also synthesized and prepared nano-ordered particles with using self-assembling systems of amphiphilic polypeptide, polydepsipeptide, and protein. Here, we overview our works on the molecular assembly systems as well as other nanocarriers, and their utilization as nano-ordered carriers for tumor imaging on the basis of the EPR effect.

## 2. Liposome and its analogues

Micellar and vesicular molecular assemblies have been prepared from various amphiphilic compounds. Liposome, which was discovered in 1964 by Bangham *et al.*,[13] is one of the most famous and widely utilized nano-carriers, and is made of the same components as cell lipid bilayer membranes. Liposome has been utilized as a nano-ordered carrier for drug delivery, since hydrophilic compounds can be encapsulated into the hollow space of liposome. There are more than ten commercially supplied liposome drugs.[14] However, there are two intrinsic problems for liposome to be used *in vivo* as a nanocarrier. One is the physical stability of liposome. Hydrophobic interactions between alkyl chains are not strong enough for a long circulation in blood stream. Some additives such as cholesterol are normally mixed to the phospholipid for the membrane stabilization. The other problem is related with bio-defense systems. In our living system, liposome is opsonized by plasma proteins, quickly recognized as a foreign particle, and likely to be captured by the cells at reticulo-endothelial system (RES) of liver and spleen. Liposome surface is therefore modified so as to obtain an escape ability, the stealth property in other words, from RES. Actually, chemical modification of liposome with hydrophilic macromolecules such as poly(ethylene glycol) (PEG) is frequently adopted to prolong *in vivo* blood clearance time. The hydrophilic surface coating prevents the surface from opsonin adsorption, resulted in reduction of liposome uptake by RES.[15] PEGylated liposomal doxorubicin, Doxil®, is a typical example of the approved medical usage of the stealth liposome. [16-18]

In order to prepare physically stable molecular assemblies, various approaches have been

examined. Connecting two or more phospholipids by covalent cross-linking bonds is one approach. For example, diacetylenes are known to be polymerized topochemically by UV irradiation at 254 nm to form a conjugated en-yne structure. Vesicular assembly was prepared from diyne-phospholipids, and was treated by the UV irradiation. The polymerized liposome shows extremely high stability against osmotic shock due to the formation of the conjugated en-yne network in the alkyl chains.[19-22]

Organic-inorganic hybrid type vesicular assembly named “cerasome” was prepared from an artificial lipid bearing a trialkoxysilylated head with a dialkyl tail. Vesicular surface of the cerasome is partially coated with silica that is derived from acid hydrolysis of the trialkoxysilylated head groups. Owing to the siloxane network on the liposomal membrane surface, cerasome is infusible. Cerasome shows high morphological stability in aqueous solution, and it can be stored at least for several months at room temperature without any change.[23,24]

These intermolecularly cross-linked molecular assemblies show high resistivity against morphological change, however, with loosing membrane fluidity and fusion ability, which are important properties for lipid membranes.

**3. Peptosome**

Vesicular assemblies consisted of amphiphilic block polymers are referred as “polymersome”.[25-29] Compared with liposome, polymersomes are physically stable due to the strong intermolecular hydrophobic interactions of the long hydrophobic block. Various synthetic amphiphilic block polymers, whose hydrophobic block was consisted of poly(styrene), poly(butadiene) and so on, have been used for polymersomes. PEG is frequently used as a hydrophilic block in the amphiphilic block polymers due to the observation that PEGylated molecular assemblies are hardly recognized by bio-defense system as discussed above.

Polypeptides are one of three major biomacromolecules, where the others are polysaccharides and nucleic acids, and are expected to show high biocompatibility and

biodegradability. Kataoka's group is a pioneer in the studies on peptide molecular assemblies and their application for drug delivery system (DDS). A cationic amphiphile and an anionic amphipile both in aqueous solutions are mixed under specified concentrations to generate vesicles with a narrow size distribution. The peptide-based polyion complex vesicle is named as PICsome, which has an advantage to avoid use of organic solvent at preparation.[30,31]

Polypeptides can be designed to take a specific conformation such as $\alpha$-helix and $\beta$-sheet, which makes molecular assemblies have a well-defined structure. We thus have explored various amphiphilic polymers having a helix segment as a hydrophobic block about their molecular assemblies. In naturally occurring proteins, several motifs composed of helices such as coiled coil and four-helix bundle are frequently found out, indicating a good packing ability of peptide helices. Further, the molecular assemblies composed of helix bundles at the hydrophobic core region will exhibit a moderate elasticity because the helix bundles may generate shear stress with accompanying morphological distortion, which is in contrast to the rigid property of polymersomes due to the chain entanglements at the hydrophobic core region. Even though some rigidity is prerequisite for nanocarriers to be delivered suitably,[32] highly rigid nanocarriers may have a concern to be stuck in very narrow blood capillaries. Nanocarriers with moderate elasticity are suitable for passing through blood capillaries, which will make *in vivo* half-life time of nanocarriers long.

### *3.1. Peptosome having a PEG chain as a hydrophilic block*

Gramicidin A (g. A), a 15 mer peptide antibiotic is known to form ion channels in lipid bilayer membranes with taking a helical structure. Gramicidin A-poly(ethylene glycol) (PEG) conjugate was found out to form vesicles with a diameter in the range of 80–90 nm by self-assembling, which was reported in 1999 and named "peptosome" (Figure 1).[33] The gramicidin A-PEG vesicles kept the vesicular morphology even at high concentrations of Triton X-100, which destroyed dimyristoylphosphatidylcholine (DMPC) liposomes. The gramicidin A blocks took a double helical structure which are tightly packed in the membrane region as illustrated in Figure 2.

Since then, several groups have reported on “peptosome”, showing possibility of peptide-based assemblies to biomedical applications.[34-42]

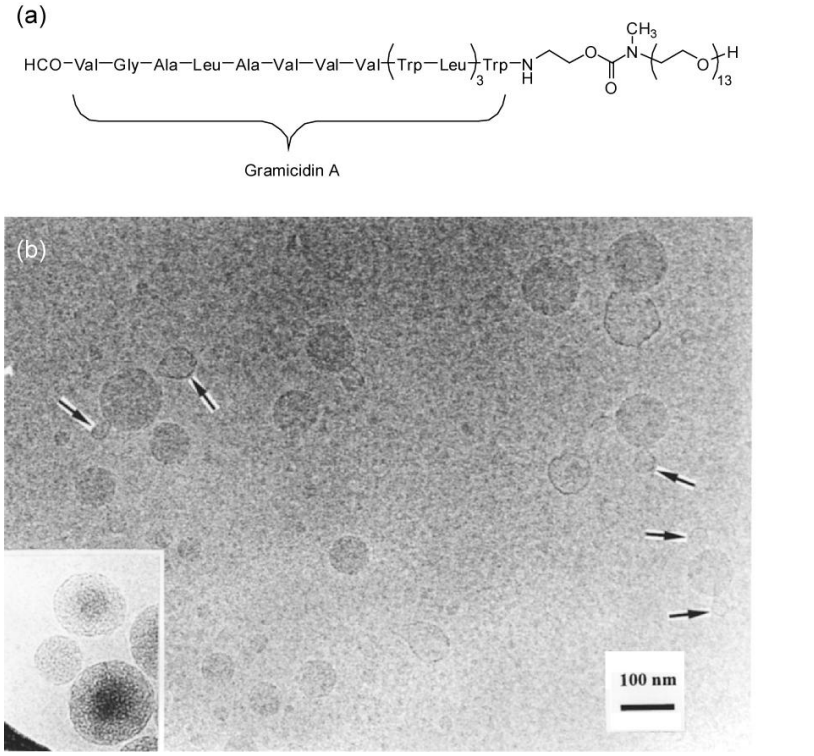


**Figure 1.** (a) Chemical structure of gramicidin A-poly(ethylene glycol) conjugate (b) Cryogenic temperature transmission electron microscope (Cryo-TEM) image of the gramicidin A-PEG assembly in water prepared by brief sonication using a probe-type sonicator. Vesicles as well as stuffed particles were observed. The stuffed particles have a multilamellar structure as shown in the inset image at the left-bottom corner (at the same magnification), which was out of focus to improve the contrast. There are several sites which show formation of unilamellar vesicles by stripping off the outer skin of the multilamellar particles (indicated by arrows). “Reprinted with permission from Reference citation 33. Copyright 1999 American Chemical Society.”

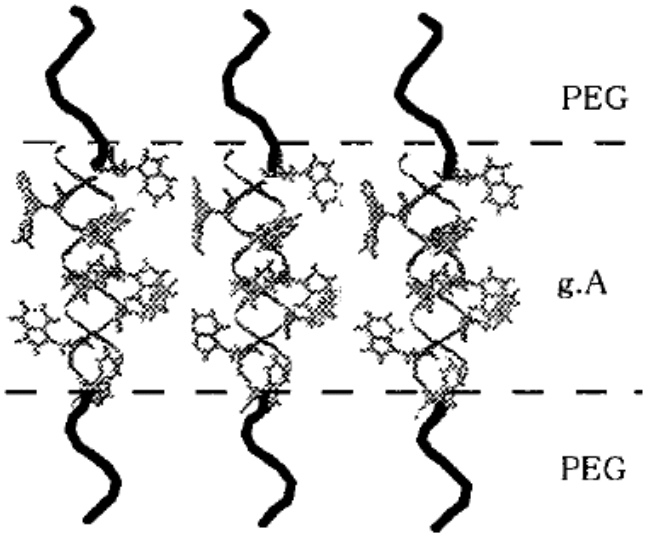


**Figure 2.** Illustration of the helix peptide membrane of the gramicidin A (g. A)-PEG vesicles. "Reprinted with permission from Reference citation 33. Copyright 1999 American Chemical Society."

*3.2. Peptosome having a disaccharide block*

PEG is allowed for medical and pharmaceutical usages. Even though PEG are regarded as biologically inert and having an escape ability from RES as described before, there are some reports on several adverse effects of PEGylated liposome on the human body, including complement activation.[43,44] PEG is an artificial synthetic macromolecule and cannot be metabolized in our living system. Therefore, an alternative choice of the hydrophilic block of PEG with a biodegradable resource is expected to be developed.

Hydrophobic helical peptide having lactose (Lac) as a hydrophilic block was synthesized and its self-assembly in water was studied.[45] Cryogenic temperature transmission electron microscope (Cryo-TEM) observation and dynamic light scattering (DLS) measurment revealed that helical 8-mer glycopeptide, Nap-(Ala-Aib)$_4$-NHCH$_2$CH$_2$NH-Lac formed vesicle in a diameter of 70 nm with a narrow distribution. On the other hand, the dodecaglycopeptide gave fibrous assembly, and the hexadecapeptide could not be dispersed in water due to the highly hydrophobic property.

Sarcosine (*N*-methyl glycine) is a naturally occurring amino acid, and the structure is a part of creatine which helps to supply energy to muscle cells. It is degraded endogeneously by sarcosine dehydrogenase, and no side effects are reported except the sarcosinaemia. Nonionic and hydrophilic poly(Sar) chain is considered to have an advantage against poly(ethylene glycol) (PEG) chain on biodegradability due to the equipped metabolic pathway for sarcosine.

Amphiphilic block polypeptide, poly(L-Glu(OMe))-*block*-poly(Sar) was synthesized using *N*-carboxyanhydride (NCA) polymerization techniques (Figure 3a).[46] According to the hydrophilic and hydrophobic balance of the block polypeptides, poly(L-Glu(OMe))-*block*-poly(Sar) gave micelle with diameter of 30–40 nm and vesicle with diameter of 100–400 nm. Circular dichroic (CD) analysis indicated that hydrophobic peptide took α-helical structure. From the transmission electron microscopy (TEM) observation of the vesicular molecular assembly, the membrane thickness was estimated about 11 nm, suggesting that the hydrophobic helices took interdigitated configuration with antiparallel orientation to stabilize the helix packing due to the dipole-dipole interaction.

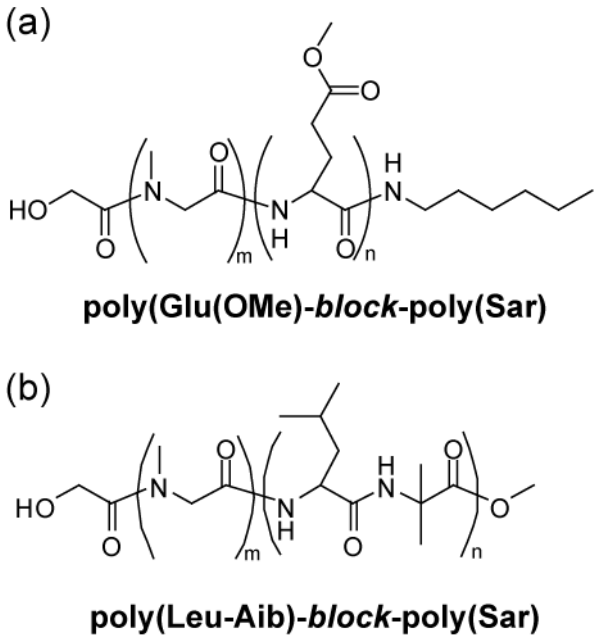


**Figure 3.** Chemical structures of (a) poly(Glu(OMe))-*block*-poly(Sar), and (b)

poly(Leu-Aib)-*block*-poly(Sar) amphiphilic polypeptide.

Both blocks of poly(L-Glu(OMe))-*block*-poly(Sar) were synthesized by a NCA polymerization method, therefore, resulting in the occurrence of polydispersity, despite of relatively small values, on their both hydrophilic and hydrophobic blocks. To avoid the polydispersity of the hydrophobic helical block, dodecapeptide of repeating Leu-Aib as a helical hydrophobic block was conjugated with poly(Sar) (Figure 3b).[47] The amphiphilic block polypeptides also gave various morphological molecular assemblies according to the hydrophilic and hydrophobic balance of the polymer. In a Tris buffered solution (10 mM, pH 7.4), $(Leu\text{-}Aib)_6$-*block*-$poly(Sar)_{27}$ formed sheet-shaped molecular assembly. The sheet was highly homogeneous in size, and the average shape was a square with a side of ca. 200 nm (Figure 4a). Upon heating the solution at 90 °C for 10 min, the sheet-shaped molecular assembly was transferred into the tubular assembly, whose diameter and length was ca. 60 nm, and ca. 200 nm, respectively (Figure 4b). The polydispersity index of the molecular assembly was lower than 0.1, indicating the highly homogenous assemblies being produced.

Heating may have induced reduction of the total area of the unstable hydrophobic edges in the sheet-shaped assembly by transformation into the tubular structure. At the open mouths of the nanotube, hydrophobic blocks of the amphiphilic peptides were exposed in the same way as the edges of the sheet-shaped structures. Therefore, the peptide nanotube is also metastable. When the peptide nanotube solution was heated at 90 °C for 24 h, the nanotubes were partly elongated to double, triple, and quadruple lengths by sticking the unstable open mouths with each other (Figure 4c). Interestingly, by mixing two amphiphilic block polypeptides having different poly(Sar) chain lengths, $(Leu\text{-}Aib)_6$-*block*-$poly(Sar)_{10}$ and $(Leu\text{-}Aib)_6$-*block*-$poly(Sar)_{27}$ (3:7 (w/w)), three way nanotube was constructed (Figure 4d).

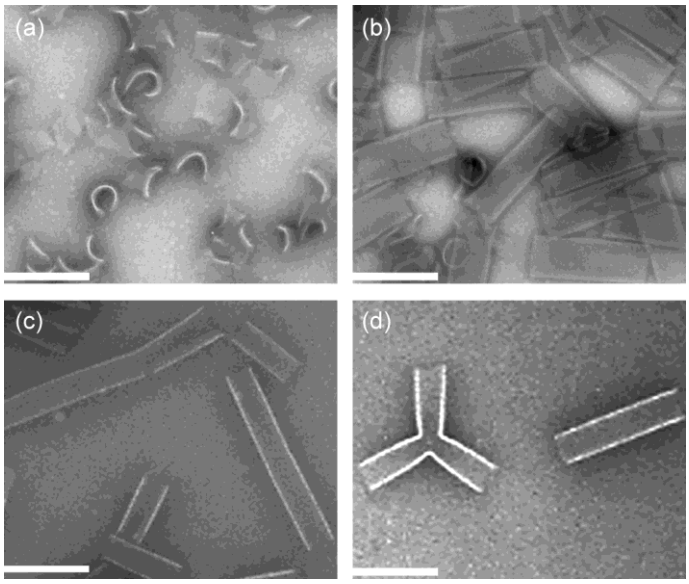


**Figure 4.** Negatively stained TEM images of the molecular assembly from (Leu-Aib)$_6$-*block*-poly(Sar)$_{27}$ (a) before heating, (b) after heating at 90 °C for 1 h, and (c) for 24 h. (d) TEM image of molecular assembly obtained from 3:7 (w/w) mixture of (Leu-Aib)$_6$-*block*-poly(Sar)$_{10}$ and (Leu-Aib)$_6$-*block*-poly(Sar)$_{27}$ after heating at 90 °C for 1 h. Bar = 200 nm. "Reprinted with permission from Reference citation 47. Copyright Wiley-VCH Verlag GmbH & Co. KGaA."

*3.3. Application of Peptosome for Tumor Imaging*

Poly(L-Glu(OMe))-*block*-poly(Sar) was labeled with near-infrared fluorescent molecule of indocyanine green (ICG), and ICG labeled molecular assembly was prepared from the 97:3 (wt/wt) mixture of non- and ICG-labeled amphiphilic polypeptides.[46] *In vivo* retention time of the ICG-labeled peptosome in rat was determined by fluorescence measurements of the residual amounts of ICG in blood plasma. The peptosome showed relatively long half-life time, which is comparable to that of PEGylated liposome under the same experimental conditions.

The ICG labeled peptosome or peptide micelle was intravenously administrated to the tumor-bearing mice and their disposition was traced using a near-infrared optical imaging system, IVIS-200 (Xenogen). In both cases, ICG-labeled molecular assemblies were gradually accumulated

in the tumor region, and the imaging contrast of the tumor region against the other healthy region became the highest after 2 or 3 days from the administration via tail vein (Figure 5), suggesting the EPR effect for the accumulation. The imaging contrast with using peptosome was better than that with using peptide micelle, because the smaller nanocarrier is leakier from blood vessels to increase the background fluorescence intensity.

Peptosome keeps vesicular morphology in blood stream, as it was shown that encapsulated water-soluble agent and the component of peptosome were delivered together to the tumor site.[46] The peptosome membrane is thus stable in blood stream, and the helix stacking makes the membrane strong enough for delivering probes and drugs to tumor sites.

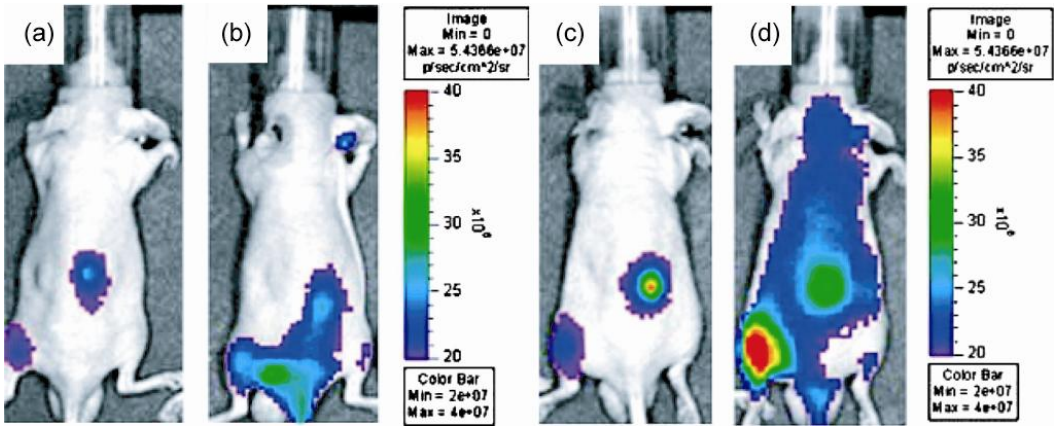


**Figure 5.** *In vivo* cancer imaging using (b) NIRF-labeled peptosome and (d) peptide micelle. ICG-labeled peptosome was prepared from a mixture of GA-poly(Sar)$_{43}$-*block*-poly(Glu(OMe))$_{18}$ and GA-poly(Sar)$_{65}$-*block*-poly(Glu(OMe))$_{18}$ (1:1) labeled with 3 wt% ICG-poly(Sar)$_{63}$-*block*-poly(Glu(OMe))$_{20}$. ICG-labeled peptide micelle was prepared from GA-poly(Sar)$_{93}$-*block*-poly(Glu(OMe))$_{12}$ labeled with 3 wt% ICG-poly(Sar)$_{63}$-*block*-poly(Glu(OMe))$_{20}$. (a, c) Bioluminescence image of SUIT2/EF-luc xenografts on the tumor-bearing mouse after administration of D-luciferin. (b, d) Image of fluorescence from ICG, 1 day after the administration of ICG-labeled peptosome, and peptide micelle, respectively. "Reprinted with permission from Reference citation 46. Copyright 2008

American Chemical Society."

In the same way with ICG labeled peptide micelle composed of poly(Glu(OMe))-block-poly(Sar), poly(Sar)-$(Leu\text{-}Aib)_8$ (the degree of polymerization of the poly(Sar) block 60) micelle with 32 nm diameter also accumulated at the transplanted tumor region (Figure 6b).[48] Therefore, peptide assemblies are considered to be effective nanocarriers for tumor imaging on the basis of the EPR effect.

**4. Lactosome**

Poly(L-lactic acid) (PLLA), which is biodegradable and biocompatible, is also known to take $3_{10}$ helical conformation. Similarly to peptosome and peptide micelle described above, amphiphilic PLLA-*block*-poly(Sar) polydepsipeptide self-assembled in aqueous solution with taking various morphologies in a dependent manner on the hydrophobic-hydrophilic balance (Figure 6a). We named the molecular assemblies composed of those depsipeptides as "Lactosome®".[49]

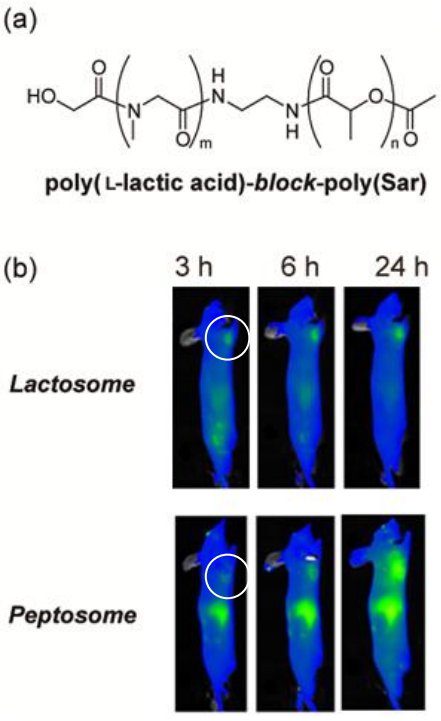

**Figure 6.** (a) Chemical structure of PLLA-*block*-poly(Sar) (the degrees of polymerization are 30 for the PLLA block and 90 for the poly(Sar) block, respectively) amphiphilic block polydepsipeptide. (b) Time lapase *in vivo* cancer imaging using ICG-labeled lactosome and Dy-776 labeled peptosome composed of poly(Sar)$_{60}$-(Leu-Aib)$_8$. 9-week-old nude mice, grafting SUIT-2/EF-Luc cells at front legs were used for the imaging. "Reprinted with permission from Reference citation 47. Copyright 2009 Elsevier."

PLLA terminal end was chemically modified with ICG.[47] By mixing 3 wt% of the ICG labeled PLLA to the non-ICG labeled PLLA-*block*-poly(Sar) (the degrees of polymerization are 30 for the PLLA block and 90 for the poly(Sar) block, respectively), ICG labeled lactosome (polydepsipeptide micelle) with diameter of 37 nm was prepared. The ICG labeled lactosome was intravenously administrated from the tail vein to the tumor-bearing mouse, and biodistribution of the fluorescent agent was traced by using optical imaging system, Clairvivo OPT (Shimadzu Corp.) (Figure 6b). Lactosome was accumulated at the transplanted tumor region within 24 hours. Importantly, uptake by RES of liver and spleen was drastically suppressed compared with ICG-labeled peptide micelle having a similar diameter. The cross section area of peptide chain with α-helical structure is about 5-fold larger than that of PLLA. Further, poly(Sar) chain length of lactosome is about 50% longer than that of peptide micelle. The hydrophilic shell of lactosome should be therefore thicker and denser than that of peptide micelle, which may be the reason for the better escape ability from the RES.

Liver tumor imaging using macromolecular nano-ordered micelle is generally considered to be difficult because the micelle is trapped at healthy liver region by RES. Liver tumor imaging with lactosome was then challenged by using the HepG2 (Human hepatocellular liver carcinoma cell line) transplanted mice. The optical images, which were taken after 48 h from the administration, showed that the ICG fluorescence site overlapped at the luciferin bioluminescence site, which was a marker of HepG2. *Ex vivo* NIRF liver image also showed that ICG fluorescence was clearly

observed at the same place with the luciferin bioluminescence (Figure 7). Despite the orthotopic transplantation, lactosome accumulated at the tumor region with high efficiency by the EPR effect. Therefore, Lactosome is considered to be a powerful candidate of nanocarriers not only for tumor imaging but also for drug delivery system.

Lactosome was also labeled by $^{18}F$ and $^{131}I$ for tumor imaging by PET and SPECT, respectively. Those labeled lactosomes are preliminarily shown to be effective for imaging of subcutaneously grafted tumors, liver tumor, pancreas tumor, colon tumor and cerebral tumor, which reports are under preparation.

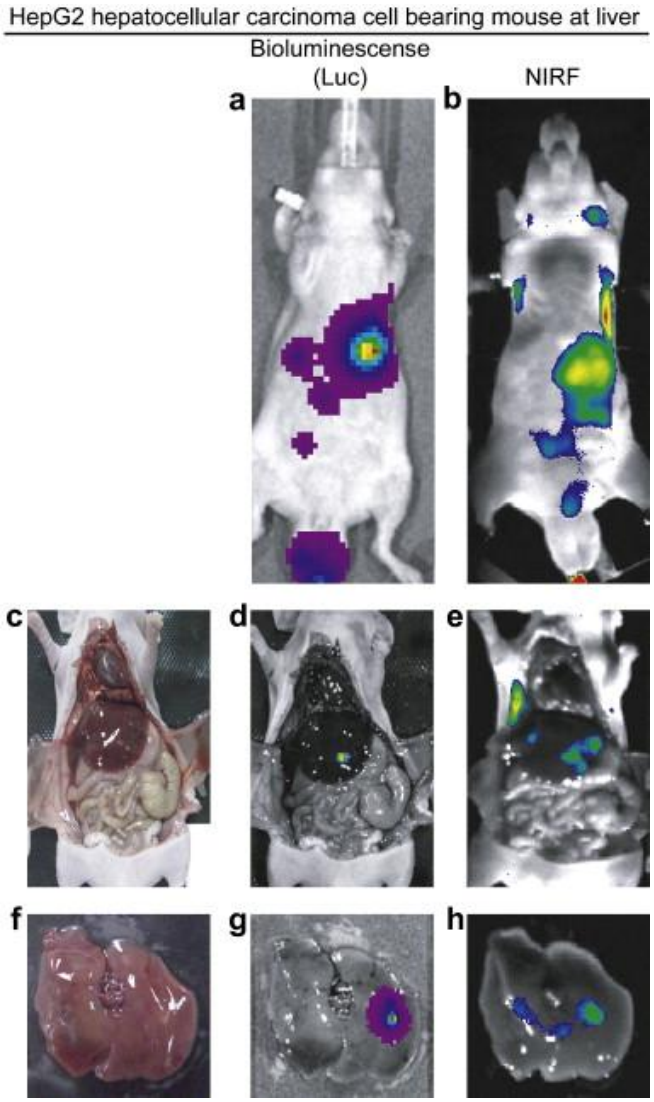


**Figure 7.** Bright field, luciferin bioluminescence, and ICG fluorescence images of HepG2

hepatocellular carcinoma cell bearing mouse at liver (a–e), and its isolated liver (f–h). Strong signal was observed from the NIRF image of tumor bearing mouse at liver (b, e, h), where is the same place with luciferin bioluminescence (a, d, g).

**5. Apoferritin (Protein Capsule)**

Protein capsules are constructed by self-assembling of protein subunits into nano-cages. Apoferritin,[50-54] viral capsids, DNA binding protein (Dps), small heat shock protein (sHsp) are well-known examples of the protein cages. Their utilization as nano-carriers for DDS and cancer imaging probe has been examined by taking advantages of their native hollow structure. There are many reactive groups on inner and outer surfaces of the protein cages, therefore, they can be easily chemically modified for functionalization.

Apoferritin is an apoprotein, which consists of 24 protein subunits of two types (heavy and light chains), and forms a hollow cage-like structure with diameter of ca. 13 nm. It can encapsulate up to 4500 iron atoms as ferric oxyhydroxide form, and works as an iron storage protein named ferritin in our living system. According to the pH conditions, the 24 protein subunits of apoferritin can associate and disassociate reversibly, and various drugs and imaging agents can be encapsulated into the cavity. Using encapsulation ability in the cavity, application of apoferritin for nanocarriers like DDS has been examined.[55,56]

Apoferritin-based MRI contrast agent is also investigated. For example, Aime *et al.* encapsulated a commercially available nonionic Gd-chelate, Gd-HPDO3A, in apoferritin cavity with using pH adjustment, and evaluated its performance as an MRI contrast agent.[57] They chemically modified the surface of the Gd-loaded apoferritin with biotin. Utilizing the biotin-streptavidin specific binding system, the biotinylated Gd-loaded apoferritin bound to a tumor region, which was pretargeted by biotinylated peptide ligand, with help of simultaneous administration of streptavidin.[58] Manganese[59] and iron[60] were also encapsulated into apoferritin cavity to be utilized as MRI contrast agents.

We also developed a Gd-chelate-condensed type MRI contrast agent in apoferritin cavity and to perform tumor specific imaging on the basis of the EPR effect. Aime's group reported that encapsulation efficiency of Gd-chelates into apoferritin was relatively low, and the amount of Gd-chelates encapsulated into each apoferritin was ca. 10.[51] We designed a new cationic Gd-chelate, Gd-$Me_2$DO2A, to improve the low yield of encapsulation. The uptake of the cationic Gd-chelate by apoferritin should be accelerated by the negative charges on the inner surface of apoferritin due to the localization of carboxylic residues (Figure 8).

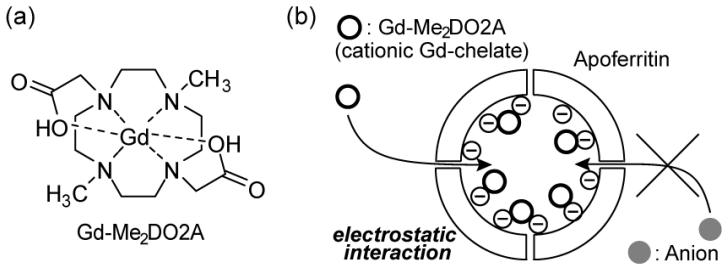


**Figure 8.** (a) Chemical structure of the newly designed cationic Gd-chelate, Gd-$Me_2$DO2A, (b) Gd-chelate condensed type MRI contrast agent in apoferritin cavity using the electrostatic interaction between cationic Gd-$Me_2$DO2A and anionic apoferritin inner surface.

Encapsulation efficiency of Gd-$Me_2$DO2A was improved as the increase of the encapsulated Gd-chelates per apoferritin from 6 for Gd-DOTA to 36 for Gd-$Me_2$DO2A under the same preparative conditions. The proton relaxivity of Gd-$Me_2$DO2A encapsulated in apoferritin was raised up to 35.9, which is ca. ten times higher than that of commercially available Gd-DOTA of 3.9 (Fgiure 9a). The high relaxivity may be explainable by two factors: 1) the increased water coordination number and 2) the reduction of the rotation correlation time, so called the macromolecular effect. The latter is consistent with our interpretation that the encapsulated cationic Gd-chelates are immobilized on the negative charges at the inner surface of apoferritin.

Apoferritin has a strong tendency to accumulate in liver by itself,[61] which is a problem for

selective delivery of the Gd-chelate-loaded apoferritin to tumor tissues by the EPR effect. To solve the problem, the apoferritin surface was modified by dextran to prolong *in vivo* blood clearance time. MR imaging using human carcinoma transplanted mice showed that dextran coated apoferritin MRI contrast agent was delivered to the tumor region by the EPR effect, and the tumor region was precisely imaged with lower dosing amount of gadolinium compared with that of commercially available Gd-chelates MRI contrast agent, Gd-DOTA.

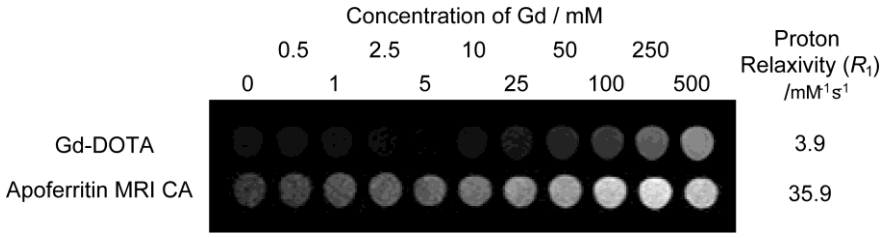


**Figure 9.** Phantom image of Gd-DOTA and Gd-$Me_2$DO2A encapsulated apoferritin MRI contrast agent.

### *6. Conclusion*

We demonstrate that amphiphilic polypeptide or polydepsipeptide having helical structures in their hydrophobic blocks form nanocarriers with high physical stability. Hydrophobic helical chains are regularly packed without chain entanglement in these molecular assemblies, resulting in showing moderate elasticity to circulate with long half time in blood stream. With controlling the hydrophilic-hydrophobic balance of the amphiphilic block polymers having a hydrophobic helical block, molecular assemblies of various morphologies, micelle, vesicle, nanotube, and three-way nanotube, are prepared.

We have applied these nanocarriers for tumor imaging. These nanocarriers show good escape ability from bio-defense systems of living organisms and circulate stably in blood stream. At tumor regions, micelles with diameter of ca. 30 nm are leaked out from the blood vessels to be remained there by the EPR effect.

Cytotoxicity of the nanocarriers and/or their degradated products is one of the most important problems to overcome for the usage of nanocarriers on drug delivery system (DDS). Our nanocarriers are prepared from biocompatible and biodegradable materials such as polypeptide and proteins, and of great advantages on medical applications.

### *7. References*


(1) see web site of World Health Organization (WHO), http://www.who.int/cancer/en/

(2) Sharkey, R. M.; Rossi, E. A.; Chang, C.-H.; Goldenberg, D. M. Cancer Biother. Radiopharm. 2010, 25, 1-12.

(3) Diagaradjane, P; Orenstein-Cardona, J. M.; Colon-Casasnovas, E.; Deorukhakar, A.; Shentu, S.; Kuno, N.; Schwartz, D. L.; Gelovani, J. G.; Krishnan, S. Clin. Cancer Res. 2008, 14, 731-741.

(4) Gong, H.; Kovar, J.; Little, G.; Chen, H.; Olive, D. M. *Neoplasia*, **2010**, *12*, 139-149.

(5) Matsumura, Y.; Maeda, H. *Cancer Res.* **1986**, *46*, 6387-6392.

(6) Lukyanov, A. N.; Hartner, W. C.; Torchilin, V. P. *J. Control. Release* **2004**, *94*, 187-193.

(7) Torchilin, V. P. *Pharm. Res.* **2007**, *24*, 1-16.

(8) Wang, J. Q.; Sui, M. H.; Fan, W. M. *Curr. Drug Metab.* **2010**, *11*, 129-141.

(9) Jarzyna, P. A.; Gianella, A.; Skajaa, T.; Knudsen, G.; Deddens, L. H.; Cormode, D. P.; Fayad, Z. A.; Mulder, W. J. M. *Wiley Interdiscip. Rev.-Nanomed. Nanobiotechnol.* **2010**, *2*, 138-150.

(10) Cherukuri, P.; Glazer, E. S.; Curleya, S. A. *Adv. Drug Deliv. Rev.* **2010**, *62*, 339-345.

(11) Svenson, S. *Eur. J. Pharm. Biopharm.* **2009**, *71*, 445-462.

(12) Mondon, K.; Gurny, R.; Moller, M. *Chimia* **2008**, *62*, 832-840.

(13) Bangham, A. D.; Horne, R. W. *J. Mol. Biol.* **1964**, *8*, 660-&.

(14) Malam, Y.; Loizidou, M.; Seifalian, A. M. *Trends Pharmacol. Sci.* **2009**, *30*, 592-599.

(15) Allen, T. M.; Hansen, C.; Martin, F.; Redemann, C.; Yauyoung, A. *Biochimica Et Biophysica Acta* **1991**, *1066*, 29-36.

(16) Immordino, M. L.; Dosio, F.; Cattel, L. *Int. J. Nanomed.* **2006**, *1*, 297-315.

(17) Gabizon, A.; Catane, R.; Uziely, B.; Kaufman, B.; Safra, T.; Cohen, R.; Martin, F.; Huang, A.; Barenholz, Y. *Cancer Res.* **1994**, *54*, 987-992.

(18) Symon, Z.; Peyser, A.; Tzemach, D.; Lyass, O.; Sucher, E.; Shezen, E.; Gabizon, A. *Cancer* **1999**, *86*, 72-78.

(19) Hub, H. H.; Hupfer, B.; Koch, H.; Ringsdorf, H. *Angew. Chem.-Int. Edit. Engl.* **1980**, *19*, 938-940.

(20) Okada, S.; Peng, S.; Spevak, W.; Charych, D. *Accounts Chem. Res.* **1998**, *31*, 229-239.

(21) Mueller, A.; O'Brien, D. F. *Chem. Rev.* **2002**, *102*, 727-757.

(22) Ringsdorf, H.; Schlarb, B.; Venzmer, J. *Angew. Chem.-Int. Edit. Engl.* **1988**, *27*, 113-158.

(23) Katagiri, K.; Ariga, K.; Kikuchi, J. *Chem. Lett.* **1999**, 661-662.

(24) Sasaki, Y.; Matsui, K.; Aoyama, Y.; Kikuchi, J. *Nat. Protoc.* **2006**, *1*, 1227-1234.

(25) Zhang, L; Eisenberg, A. *Science* **1995**, *268*, 1728-1731.

Cornelissen, J. J. L. M.; Fischer, M.; Sommerdijk, N. A. J.; Nolte, R. J. M. *Science*, **1998**, *280*, 1427-1430.

(26) Discher, B. M.; Hammer, D. A.; Bates, F. S.; Discher, D. E. *Curr. Opin. Colloid Interface Sci.* **2000**, *5*, 125-131.

(27) Discher, D. E.; Eisenberg, A. *Science* **2002**, *297*, 967-973.

(28) Lensen, D.; Vriezema, D. M.; van Hest, J. C. M. *Macromol. Biosci.* **2008**, *8*, 991-1005.

van Dongon, S. F. M.; Nallani, M.; Schoffelen, S.; Cornelissen, J. L. M.; Nolte, R. J. M.; van Hest, J. C. M. *Macromol. Rapid. Commun.* **2008**, *29*, 321-325.

(29) Christian, D. A.; Cai, S.; Bowen, D. M.; Kim, Y.; Pajerowski, J. D.; Discher, D. E. *Eur. J. Pharm. Biopharm.* **2009**, *71*, 463-474.

(30) Koide, A.; Kishimura, A.; Osada, K.; Jang, W. D.; Yamasaki, Y.; Kataoka, K. *J. Am. Chem. Soc.* **2006**, *128*, 5988-5989.

(31) Anraku, Y.; Kishimura, A.; Oba, M.; Yamasaki, Y.; Kataoka, K. *J. Am. Chem. Soc*. **2010**, *132*, 1631-1636.

(32) Inokuchi, Y.; Hironaka, K.; Fujisawa, T.; Tozuka, Y.; Tsuruma, K.; Shimazawa, M.; Takeuchi, H.; Hara, H. *Invest. Ophthalmol. Vis. Sci.* **2010**, *51*, 3162-3170.

(33) Kimura, S.; Kim, D. H.; Sugiyama, J.; Imanishi, Y. *Langmuir* **1999**, *15*, 4461-4463.

(34) Checot, F.; lecommandoux, S.; Gnanou, Y.; Klok, H.-A. *Angew. Chem. Int. Ed*. **2002**, *41*, 1340-1343.

(35) Kukula, H.; Schlaad, H.; Antonietti, M.; Foerster, S. *J. Am. Chem. Soc*. **2002**, *124*, 1658-1663.

(36) Checot, F.; Lecommandoux, S.; Klok, H.-A.; Gnanou, Y. *Eur. Phys. J. E* **2003**, *10*, 25-35.

(37) Bellomo, E. G.; Wyrsta, M. D.; Pakstis, L; Pochan, D. J.; Deming, T. J. *Nature Mat*. **2004**, *3*, 244-248.

(38) Rodriguez-Hermandez, J.; Lecommandoux, S. J. *Am. Chem. Soc*. **2005**, *127*, 2026-2027.

(39) Koning, R. I.; Kros, A. *J. Am. Chem. Soc*. **2009**, *131*, 13186-13187.

(40) Guo, B.; Shi, Z; Yao, Y.; Zhou, Y.; Yan, D. *Langmuir* **2009**, *25*, 6622-6626.

(41) Bertin, A; Hermes, F.; Schlaad, H. *Adv. Polym. Sci*. **2010**, *224*, 167-195.

(42) Versluis, F.; Tomatsu, I.; Kehr, S.; Fregonese, C.; Tepper, A. W. J. W.; Stuart, M. C. A.; Ravoo, B. J.; Cavalli, S.; Albericio, F.; Kros, A. *Chem. Soc. Rev*. **2010**, *39*, 241-263.

(43) Hamada, I.; Hunter, A. C.; Szebeni, J.; Moghimi, S. M. *Mol. Immunol.* **2008**, *46*, 225-232.

(44) Pabby, A.; Ahmed, R. *Am. J. Gastroenterol.* **2006**, *101*, 914.

(45) Kimura, S.; Muraji, Y.; Sugiyama, J.; Fujita, K.; Imanishi, Y. *J. Colloid Interface Sci.* **2000**, *222*, 265-267.

(46) Tanisaka, H.; Kizaka-Kondoh, S.; Makino, A.; Tanaka, S.; Hiraoka, M.; Kimura, S. *Bioconjugate Chem.* **2008**, *19*, 109-117.

(47) Kanzaki, T.; Horikawa, Y.; Makino, A.; Sugiyama, J.; Kimura, S. *Macromol. Biosci.* **2008**, *8*, 1026-1033.

(48) Makino, A.; Kizaka-Kondoh, S.; Yamahara, R.; Hara, I.; Kanzaki, T.; Ozeki, E.; Hiraoka, M.; Kimura, S. *Biomaterials* **2009**, *30*, 5156-5160.

(49) Makino, A.; Yamahara, R.; Ozeki, E.; Kimura, S. *Chem. Lett.* **2007**, *36*, 1220-1221.

(50) Trikha, J.; Theil, E. C.; Allewell, N. M. ; *J. Mol. Biol.* **1995**, *248*, 949-967.

(51) Harrison, P. M.; Arosio, P. *Biochim. Biophys. Acta-Bioenerg.* **1996**, *1275*, 161-203.

(52) Ilari, A.; Stefanini, S.; Chiancone, E.; Tsernoglou, D. *Nat. Struct. Biol.* **2000**, *7*, 38-43.

(53) Liu, X. F.; Theil, E. C. *Accounts Chem. Res.* **2005**, *38*, 167-175.

(54) Toussaint, L.; Bertrand, L.; Hue, L.; Crichton, R. R.; Declercq, J. P. *J. Mol. Biol.* **2007**. *365*, 440-452.

(55) Yan, F.; Zhang, Y.; Yuan, H. K.; Gregas, M. K.; Vo-Dinh, T. *Chem. Commun.* **2008**, 4579-4581.

(56) Yang, Z.; Wang, X. Y.; Diao, H. J.; Zhang, J. F.; Li, H. Y.; Sun, H. Z.; Guo, Z. J. *Chem. Commun.* **2007**, 3453-3455.

(57) Aime, S.; Frullano, L.; Crich, S. G. *Angew. Chem.-Int. Edit.* **2002**, *41*, 1017-+.

(58) Crich, S. G.; Bussolati, B.; Tei, L.; Grange, C.; Esposito, G.; Lanzardo, S.; Camussi, G.; Aime, S. *Cancer Res.* **2006**, *66*, 9196-9201.

(59) Kalman, F. K.; Geninatti-Crich, S.; Aime, S. *Angew. Chem.-Int. Edit.* **2010**, *49*, 612-615.

(60) Bryant, L. H.; Brechbiel, M. W.; Wu, C. C.; Bulte, J. W. M.; Herynek, V.; Frank, J. A. *JMRI-J. Magn. Reson. Imaging* **1999**, *9*, 348-352.

(61) Osterloh, K.; Aisen, P. *Biochim. Biophys. Acta* **1989**, *1011*, 40-45.